Fictitious Domain Method for Unsteady Problems: Application to Electromagnetic Scattering

Francis Collino, Patrick Joly, Florence Millot

INRIA

INSTITUT NATIONAL DE RECHERCHE EN INFORMATIQUE ET EN AUTOMATIQUE

Fictitious Domain Method for Unsteady Problems: Application to Electromagnetic Scattering

Francis Collino , Patrick Joly et Florence Millot

N° 2963

Août 1996

THÈME 4

ISSN 0249-6399

INRIA
ROCQUENCOURT

Fictitious Domain Method for Unsteady Problems: Application to Electromagnetic Scattering

Francis Collino*†, Patrick Joly*†et Florence Millot†

Thème 4 — Simulation et optimisation
de systèmes complexes
Projet Ondes

Rapport de recherche no2963 — Août 1996 — 46 pages

Abstract: In this work, we present and implement a fictitious domain method for time dependent problems of scattering by obstacles. We focus our attention on the case of 2D electromagnetic waves and perfectly conducting boundaries. Such a method allows us to work with uniform meshes for the electric field, independently of the geometry of the obstacle, the boundary condition being taken into account via the introduction of a Lagrange multiplier that can be interpreted as a surface current. After a brief description of the method and a presentation of its main properties, we show the superiority in terms of accuracy of this new method over the method that consists in using a staircase like approximation of the boundary

Key-words: Fictitious Domain Method, computational electromagnetics

(Résumé : tsvp)

This work has been done at CERFACS, 42 avenue G. Coriolis 31057, Toulouse. This paper has been submited to Journal of Computational Physics

* INRIA
† **CERFACS**

Unité de recherche INRIA Rocquencourt
Domaine de Voluceau, Rocquencourt, BP 105, 78153 LE CHESNAY Cedex (France)
Téléphone : (33 1) 39 63 55 11 – Télécopie : (33 1) 39 63 53 30

Méthode de domaines fictifs pour les problèmes instationnaires: Application à la diffraction des ondes électromagnétiques

Résumé : Nous présentons et analysons une méthode de domaines fictifs pour le calcul de la diffraction des ondes électromagnétiques par des obstacles conducteurs. Cette méthode consiste a prolonger le champ à l'intérieur des conducteurs et à introduire une variable supplémentaire (le courant surfacique) pour prendre en compte la condition de conducteur parfait. Son avantage est de permettre d'utiliser une grille régulière, indépendante de la géométrie des obstacles, pour le calcul du champ. Nous montrons à l'aide d'expériences numériques l'amélioration en précision obtenue par rapport à une méthode classique (approximation en marches d'escalier des surfaces conductrices).

Mots-clé : Méthode de domaines fictifs, Calcul d'ondes électromagnétiques,

1 Introduction

In recent years, solving time dependent problems of scattering by an obstacle has received considerable attention. Among the various techniques that have been studied, the finite difference method is one of the most attractive. This method uses a regular grid with an explicit scheme in time and hence is very efficient from the computational point of view. However its great disadvantage is that it creates **numerical diffraction** when the obstacle boundary does not fit the grid mesh (see Fig 1).

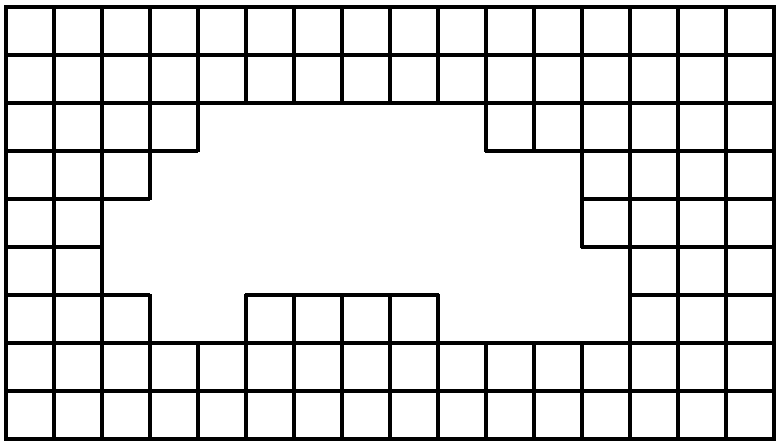

Fig 1: *Geometry of the problem*

A possibility for avoiding this drawback is to use a finite element method. The finite element mesh may follow exactly the boundary of the object (see Fig

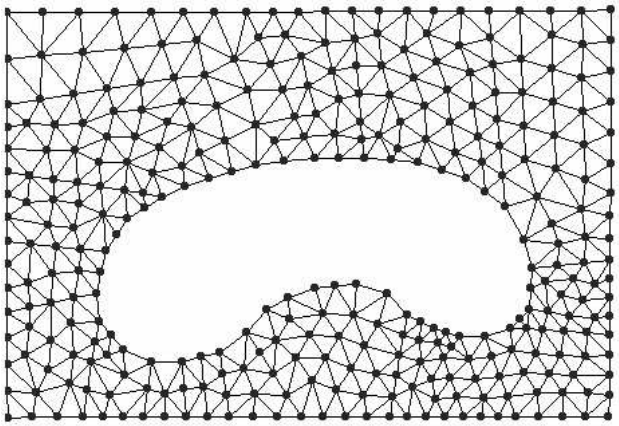

2).

Fig 2: *Example of the conformous finite element mesh in 2D*

Nevertheless, other drawbacks are introduced. It appears **necessary to use mass lumping** to obtain an explicit scheme but this is still a **difficult** to do in the case of **higher order** finite element methods ([7]) especially for **Maxwell's equations**. Further, **the numerical implementation is much more difficult** and the efficiency of the computations is decreased by the unstructured nature of the data. Finally, meshing the boundary of the obstacle may induce meshes of small size and meshing the whole domain of computation with tetrahedrons is not an easy task. Moreover the time step having to be chosen in accordance with the grid mesh size (C.F.L. condition), this may sometimes lead to small time steps.

In this paper, we investigate an alternative method for handling the scattering problem, namely the fictitious domain method. Such methods have been shown recently to have interesting potential for solving complicated problems [1] [2] [3] [19] [12] [15], particularly in the stationary case. The study of the fictitious domain method for time dependent problems has just started [16]. But we think that it should reveal really efficient for this kind of problems, especially for wave propagation problems in exterior problems, in other words for scattering by obstacles, which we intend to demonstrate in this paper. The fictitious domain method, also called the domain embedding method, consists in extending artificially the solution inside the obstacle so that the new domain of computation has a very simple shape (typically a rectangle in 2D). This extension requires the introduction of a **new variable defined only at**

the boundary of the obstacle. This auxiliary variable allows one to **take into account the boundary condition**. It can be related to a singularity across the boundary of the obstacle of the extended function. This idea will be developed in section 2. The main point is that **the mesh for the solution** on the enlarged domain can be **chosen independently of the geometry of the obstacle**. In particular, the use of regular grids or structured meshes allows for simple and efficient computations. Of course, we have to pay for this advantage in terms of some additional computational cost due to the determination of the new boundary unknown. However, the final numerical scheme appears to be a slight perturbation of the scheme for the problem without obstacle so that **this cost may be considered as marginal**. From the theoretical point of view, the convergence of the method is linked to obtaining a uniform inf-sup condition which leads to a compatibility condition between the boundary mesh and the uniform mesh [14]. Another important point is that the stability condition of the resulting scheme is the same as the one of the finite difference scheme. Practically, it implies that the two mesh grids can not be chosen completely independently, but this is not a real constrain.

The remainder of this article is divided into four sections. In section 2, we introduce the fictitious domain method for acoustic wave propagation with Dirichlet boundary conditions. We describe the formulation of the new problem. We present the space and time discretization of this problem. Some remarks about error estimates are done. We investigate also the stability of the numerical scheme. In section 3, we apply the method for the time dependent Maxwell equations. We present a new formulation of the electromagnetic scattering problem. The space and time discretization are also discussed. Some numerical results are presented and discussed in section 4. We show the superiority of the fictitious method in terms of accuracy and memory space over the method that consists in using a staircase like approximation of the boundary. The first appendix gives some comments in order to establish errors estimates. The second appendix is devoted to a very simple monodimensional analysis which demonstrates in this case the superiority of the fictitious domain method.

2 A fictitious domain method for an acoustic problem

2.1 Presentation of the method

2.1.1 Formulation of the new problem

We consider first the scattering of a wave by an obstacle $\mathcal{O}$, $\mathcal{O} \subset \mathbf{R}^d$ with $d = 2$ or $d = 3$. The solution is governed by the wave equation in D, the open complement of the obstacle with a Dirichlet condition on the boundary (see Fig 3):

$$\begin{cases} \dfrac{\partial^2 u}{\partial t^2} - \Delta u = 0 & \text{in } D \\ u = 0 & \text{on } \gamma = \partial D. \end{cases} \tag{1}$$

The incident wave is generated by initial conditions at time $t = 0$ given by

$$u(x,0) = u_0(x) \in H^1(D), \qquad \frac{\partial u}{\partial t}(x,0) = u_1(x,0) \in L^2(D). \tag{2}$$

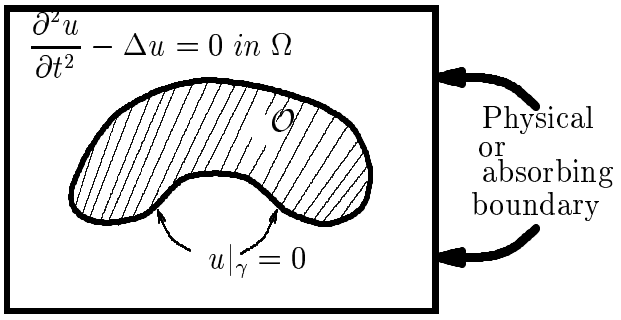

Fig 3: *Geometry of the problem*

In order to have a finite computational domain, the classical technique consists in bounding the domain D and in imposing absorbing conditions on the exterior boundary ([17], [11] [8]). For the sake of simplicity, a Dirichlet condition is assumed on the exterior boundary as well. For our purpose, we choose the geometry of the external boundary to be rectangular. We denote by Ω this bounded domain and by C the rectangle $\Omega \bigcup \mathcal{O}$ (see Fig 3). We want

to solve the simple problem described by equation (1) by the fictitious domain method. Note that this method can be used also for more complicated problems as scattering of an acoustic or electromagnetic wave in a heterogeneous medium.
The main idea of the fictitious domain method is to extend u from Ω to the enlarged domain C to a function (still denoted by u for simplicity) with $H^1(C)$ regularity. Note that this regularity requirement implies the continuity of the trace of u across the boundary.

More precisely, we look for u in the space

$$u \in \tilde{V} = \left\{ v \in H^1(C);\ v = 0 \quad on \quad \gamma \right\}, \tag{3}$$

and we define u as the first argument of (u, λ) the solution of the following variational evolution problem

$$\begin{cases} \dfrac{d^2}{dt^2}(u, v) + a(u, v) = b(v, \lambda) & \forall v \in X \\ b(u, \mu) = 0 & \forall \mu \in M, \end{cases} \tag{4}$$

where $X = H_0^1(C)$ and $M = H^{-1/2}(\gamma)$. We introduce $H = L^2(C)$ so that X is densely and continuously embedded in H and denote by $(.,.)$ the scalar product in H

$$(u, v) = \int_C uv\, dx \tag{5}$$

and the bilinear form $a(u, v)$ by

$$a(u, v) = \int_C \nabla v \nabla u\, dx \tag{6}$$

which is continuous and coercive in the space X. The bilinear form $b(u, \mu)$ denotes the duality pairing between $H^{-1/2}(\gamma)$ and $H^{1/2}(\gamma)$ and is equal to

$$b(u, \mu) = \langle \mu, u \rangle_\gamma. \tag{7}$$

We note by$| \ . \ |$,$\| \ . \ \|_X$ and $\| \ . \ \|_M$ the respective norms in H,X and M. We have

$$|v| \leq \|v\|_X = \sqrt{|v| + a(v, v)}\ \forall v \in X \tag{8}$$

In its principle, the fictitious domain method consists in extending the solution in the enlarged computational domain and to introduce a new unknown at the boundary. Its main difference between this approach and a standard conforming finite element approach lies in the fact that the Dirichlet condition is taken into account in a weak sense instead of being imposed in the functional space. It has a relationship with other approaches as we are going to see in the next two sections.

2.1.2 A justification of (4) via minimization problems

To understand (4), we can for instance consider the time t as a parameter and the function $f = -\dfrac{\partial^2 u}{\partial t^2}$ as a data. We have to solve now the following problem

$$\begin{cases} -\Delta u = f & \text{in } \Omega \\ u = 0 & \text{on } \gamma. \end{cases} \tag{9}$$

It is equivalent to minimize the functional $J(v) = int_C(\dfrac{1}{2}\|\nabla v|^2 - fv)\,dx$ over the set V of functions of $H^1(|\Omega)$ satisfying the constraint $v = 0$ on γ. The functions belonging to V can be seen as the restrictions of functions of the set $\tilde{V}$ defined in (3). It is natural to consider the enlarged minimization problem defined by

$$\min_{\tilde{v}\in\tilde{V}} J(\tilde{v}) = \int_C (\frac{1}{2}|\nabla\tilde{v}|^2 - \tilde{f}\tilde{v})\,dx \tag{10}$$

where for instance $\tilde{f} = 0$ on $\mathcal{O}$ and $\tilde{f} = f$ on Ω. It is easy to verify that the restriction of the solution of problem (10) to Ω is exactly the solution of the problem (4), that we are looking for. Problem (4) is a minimization problem with a equality constraint. Its solution is the first argument of the saddle point of the Lagrangian functional defined by $L(v,\mu) = J(v) - b(v,\mu)$. Writing that the derivative of this Lagrangian is equal to zero at the optimum (u,λ), we

obtain:

$$\begin{cases} a(u,v) = b(v,\lambda) + (f,v) & \forall v \in X \\ b(u,\mu) = 0 & \forall \mu \in M \end{cases} \tag{11}$$

which gives exactly the equations of (4) if we have written $f = -\dfrac{\partial^2 u}{\partial t^2}$.
Thus the auxiliary unknown λ of problem (4) appears as the associated Lagrange multiplier.

2.1.3 An analogy with integral equations methods

Another way to understand the system of equations (4) is to say that having extended u by continuity across γ and assuming that u still satisfies the wave equation inside $\mathcal{O}$ (this means that u solves the homogeneous Dirichlet problem inside and outside), we have in the sense of distributions on C

$$\frac{\partial^2 u}{\partial t^2} - \Delta u = \left[\frac{\partial u}{\partial n} \right]_\gamma \delta_\gamma. \tag{12}$$

where δ_γ is the surface measure supported on γ. Then, it is not difficult to reinterpret λ as being the jump of the normal derivative of u across γ. This establishes an analogy between the fictitious domain method and the integral equations for scattering problems [5]. Indeed in this kind of method, λ is typically the quantity that is chosen as the unknown. Nevertheless let us point out a very important difference between our approach and these methods. Indeed integral equations are known to lead, after discretization, to the solution of full linear systems in λ. This will not be the case for the fictitious domain method as it will be emphasized later.

In the following, we will discuss a finite element approximation of problem (4) and its time discretization.

2.2 Finite element approximation and time discretization

2.2.1 Space discretization

Let X_h (resp M_h) be a finite dimensional subspace of X (resp $H^{-1/2}(\gamma)$). We approximate the variational problem (4) by

$$\left\{ \begin{array}{l} \text{Find } u_h \in X_h, \quad \lambda_h \in M_h \quad \text{such that} \\ \dfrac{d^2}{dt^2}(u_h, v_h) + a(u_h, v_h) = b(v_h, \lambda_h) \quad \forall v_h \in X_h \\ b(u_h, \mu_h) = 0 \qquad\qquad\qquad\qquad \forall \mu_h \in M_h \end{array} \right. \tag{13}$$

Spaces X_h and M_h can be taken "independent" from each other. More precisely, X_h can be a finite element space based on a regular mesh in C (for example squares in 2D see Fig 4). X_h can be described by P1 or Q1 finite elements. On the other hand, M_h is directly related to the geometry of γ and can be for instance discretized into segments for 2D problems (see Fig 4). Of course, X_h and M_h will be supposed to satisfy the usual approximation properties

$$\left\{ \begin{array}{l} \lim\limits_{h \to 0} \inf\limits_{(v_h \in X_h)} \|u - v_h\|_X = 0 \quad \forall u \in X \\ \lim\limits_{h \to 0} \inf\limits_{(\mu_h \in X_h)} \|\mu - \mu_h\|_M = 0 \quad \forall \mu \in M. \end{array} \right. \tag{14}$$

which will be the case in the examples we shall consider later.

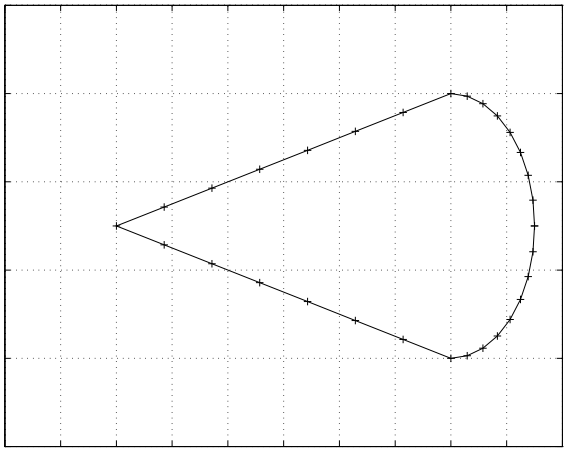

Fig 4: *Example of the two meshes in 2D*

Here, remembering that M_h is a subspace of $H^{-1/2}(\gamma)$, it makes sense to use discontinuous functions to construct X_h and then use, for instance, piecewise constant functions.

Let us introduce $\{v_j,\ 1 \leq j \leq p = \dim X_h\}$ and $\{w_\ell, 1 \leq \ell \leq q = \dim M_h\}$ two bases for the spaces X_h and M_h respectively. Indeed , we shall have respectively, if h denotes the space size of the meshes

$$\begin{cases} p = O(\frac{1}{h^2}) \quad \text{and} \quad q = O(\frac{1}{h}) \quad \text{if d =2} \\ p = O(\frac{1}{h^3}) \quad \text{and} \quad q = O(\frac{1}{h^2}) \quad \text{if d =3} \end{cases} \tag{15}$$

Let us define

- M_h = the $p \times p$ mass matrix associated to the scalar product (u_h, v_h) $(M_h \in \mathcal{L}(X_h, X_h))$
- A_h = the $p \times p$ stiffness matrix associated to the bilinear form $a(u_h, v_h)$ $(A_h \in \mathcal{L}(X_h, X_h))$
- B_h= the $p \times q$ "boundary" matrix associated to the bilinear form $b(u_h, \mu_h)(B_h \in \mathcal{L}(M_h, X_h))$

If U_h (resp Λ_h) is the column vector representing the decomposition of u_h (resp. λ_h) on the base $\{v_j\}$ (resp. $\{w_\ell\}$), we have

$$\begin{cases} M_h \dfrac{d^2 U_h}{dt^2} + A_h U_h = B_h \Lambda_h \\ B_h^t U_h = 0 \end{cases} \tag{16}$$

where B_h^t is the transpose of B_h. If M_h and A_h can be interpreted respectively as approximations of the identity and Laplace operators, B_h^t can be seen as a discrete trace operator from X_h to M_h. Note that problem (16) appears as a system of ordinary differential equations with an algebraic constraint. This establishes an analogy with problems of fluid dynamics in the incompressible case where the free divergence is the constrain.

Remark : In the following, the elements of the mass matrix M_h are supposed to be calculated via an appropriate quadrature formula in such a way that M_h becomes diagonal (mass lumping). For lower Lagrange elements, such a procedure is well known. The case of higher order elements can be handed using the ideas developed in [7]. So using mass lumping, we thus obtain an explicit scheme as we will see below.

2.2.2 Time discretization

For time discretization, the interval of time $[0, T]$ is divided into N pieces of length $\Delta t = \frac{T}{N}$. Time step Δt must be chosen in accordance with the space step of the mesh defined on the computational domain in order to satisfy the stability conditions as it will be seen later. We use a three time step finite difference explicit scheme for the time derivatives. So, problem (16) is equivalent to

$$\begin{cases} U_h^{n+1} - 2U_h^n + U_h^{n-1} = -\Delta t^2 M_h^{-1} A_h U_h^n + \Delta t^2 M_h^{-1} B_h \Lambda_h^n & (1) \\ B_h^t U_h^n = 0. & (2) \end{cases} \tag{17}$$

To compute the solution explicitly, an apparent difficulty appears with the condition $B^t U_h^n = 0$. In fact for practical computation, this condition is repla-

ced by an equivalent condition which results from multiplying the first equation by B_h^t. We obtain

$$\begin{cases} B_h^t(U_h^{n+1} - 2U_h^n + U_h^{n-1}) = -\Delta t^2 B_h^t M_h^{-1} A_h U_h^n + \Delta t^2 B_h^t M_h^{-1} B_h \Lambda_h^n & (1) \\ U_h^{n+1} = 2U_h^n - U_h^{n-1} - (\Delta t)^2 M_h^{-1} A_h U_h^n + (\Delta t)^2 M_h^{-1} B_h \Lambda_h^n & (2) \end{cases} \tag{18}$$

Because equation (2) of system (17) holds at each time, the left side of equation (1) of system (18) vanishes. Finally, we obtain the system

$$\begin{cases} U_h^{n+1} = 2U_h^n - U_h^{n-1} - (\Delta t)^2 M_h^{-1} A_h U_h^n + (\Delta t)^2 M_h^{-1} B_h \Lambda_h^n \\ B_h^t M_h^{-1} B_h \Lambda_h^n = B_h^t M_h^{-1} A_h U_h^n. \end{cases} \tag{19}$$

Reciprocally, multiplying the first equation of system (19) and using equation (2) of system (19) leads to

$$\begin{cases} U_h^{n+1} = 2U_h^n - U_h^{n-1} - (\Delta t)^2 M_h^{-1} A_h U_h^n + (\Delta t)^2 M_h^{-1} B_h \Lambda_h^n \\ B_h^t(U_h^{n+1} - 2U_h^n + U_h^{n-1}) = 0. \end{cases} \tag{20}$$

If we suppose that at initial times (n=0,n=1) the condition $B_h^t U_h^n = 0$ holds, by induction over n, it is easy to see that the condition $B_h^t U_h^n = 0$ is true at each time. So system (19) implies system (17).
In conclusion , systems (17) and (19) are equivalent as soon as we have at initial times

$$B_h^t U_h^0 = B_h^t U_h^1 = 0 \tag{21}$$

which is in fact nothing but a compatibility condition between boundary and initial conditions.
Finally, let us assume (U_h^{n-1}, U_h^n) to be known; then (U_h^n, U_h^{n+1}) is computed by the following procedure:

- first, solve equation $B_h^t M_h^{-1} B \Lambda_h^n = B_h^t M_h^{-1} A_h U_h^n$ to get the Lagrange multiplier Λ_h^n,
- second, get the wave solution at instant $n+1$ via ((19)-(1)).

Remark: another way [9] to solve problem (17) is to say that without the obstacle in the domain C, the discretized wave propagation equation is

$$U_{h,FDTD}^{n+1} = 2U_h^n - U_h^{n-1} - (\Delta t)^2 M_h^{-1} A_h U_h^n, \tag{22}$$

and the presence of the obstacle only introduces a new unknown which can be computed by the following equation

$$-(\Delta t)^2 B_h^t M_h^{-1} B_h \Lambda_h^n = B_h^t U_{h,FDTD}^{n+1}, \tag{23}$$

and perturbs the discretized wave propagation by introducing a source term as following

$$U_h^{n+1} = U_{h,FDTD}^{n+1} + (\Delta t)^2 M_h^{-1} B_h \Lambda_h^n \tag{24}$$

For the computation of the Lagrange multiplier, we must invert the matrix $Q = B_h^t M_h^{-1} B_h$. In the following, we make some remarks about this matrix.

2.3 Properties of the matrix Q

The following properties of the matrix $Q = B_h^t M_h^{-1} B_h$ are immediate,

- Q is symmetric and positive.
- The size of Q is exactly (q, q) which is very small compared to the size of matrix A_h since in practice we have $q << p$.
- Q is a sparse matrix with narrow bandwidth (see section 4.2).

Thus, if Q^{-1} exists, the inversion of Q can be performed by a Cholesky factorization or by a conjugate gradient algorithm. There remains the crucial question of the existence of this inverse. Definiteness of Q is ensured as soon as the kernel of the matrix B_h is equal to 0. This is related to a property of the continuous variational problem. More precisely, the key condition for the existence of the multiplier λ in the variational formulation (4) is the inf-sup condition,

$$\inf_{(\lambda \in M)} \sup_{(v \in X)} \frac{b(v, \lambda)}{\|\lambda\|_M \|v\|_X} = C > 0. \tag{25}$$

Similarly, the existence of (u_h, λ_h) and the convergence of the method when h tends to zero is linked to the uniform discrete inf-sup condition,

$$\exists\, C', \text{ independent of } h \text{ such that } \quad \inf_{(\lambda \in M_h)} \sup_{(v \in X_h)} \frac{b(v,\lambda)}{\|\lambda\|_M \|v\|_X} = C' > 0 \ . \quad (26)$$

This condition requires a compatibility relation between the two meshes. It imposes a condition between the dimensions of the two spaces X_h and M_h. Such a condition can be found in [14] where elliptic problems are studied. More precisely, it is demonstrated theoritically that if the space increment h_s used for the discretization of the obstacle is three times larger than the space increment h_v used for the regular squared mesh, the uniform inf-sup condition holds. However numerical experiments show that this condition can be relaxed from 3 to a number slightly larger than one. In any case, h_v must be smaller than h_s. In consequence, for a given space increment, it is impossible to use the fictitious domain method for obstacles whose geometry is too much irregular with respect to h_v.

2.4 About error estimates

We want here to estimate the error between the approximate solution (u_h, λ_h) of the semidiscrete problem (13) and the exact solution (u, λ) of problem (4) provided that this solution is regular enough. To do so, we suppose that the uniform discrete condition (26) is fulfilled. Following Dupont [10] or Brezzi [6], we introduce the elliptic operator defined from $X \times M$ to $X_h \times M_h$ by

$$\Pi_h(u, \lambda) = (\Pi_h u, \Pi_h \lambda), \quad \text{and} \quad (27)$$

$$\begin{cases} a(u - \Pi_h u, v_h) = b(v_h, \lambda - \Pi_h \lambda) & \forall v_h \in X_h \\ b(u - \Pi_h u, \mu_h) = 0 & \forall \mu_h \in M_h. \end{cases} \quad (28)$$

It can be shown [6] that the uniform inf-sup condition joined to the coercivity of the bilinear form a ensures the existence and the uniqueness of Π_h.

Using Π_h, the error between the approximate solution and the exact solution is split into two parts

$$\left\{\begin{array}{lll} u-u_h(t) = & (u(t)-\Pi_h u(t))+(\Pi_h u(t)-u_h(t)) & = \epsilon_h(t)+\eta_h(t) \\ \lambda-\lambda_h(t) = & (\lambda(t)-\Pi_h\lambda(t))+(\Pi_h\lambda(t)-\lambda_h(t)) & = \theta_h(t)+\tau_h(t). \end{array}\right. \tag{29}$$

Let us set

$$\|(u,\lambda)-\Pi_h(u,\lambda)\| = \|u(t)-\Pi_h u(t)\|_X + \|\lambda(t)-\Pi_h\lambda(t)\|_M, \tag{30}$$

we have the classical result

$$\left\{\begin{array}{l} \exists\,\sigma, \text{ independent of } h \text{ such that} \\ \\ \|(u,\lambda)-\Pi_h(u,\lambda)\| \le \sigma\left\{\inf_{v_h\in X_h}\|u(t)-v_h\|_X + \inf_{\mu_h\in M_h}\|\lambda(t)-\mu_h\|_M\right\}, \end{array}\right. \tag{31}$$

which shows thanks to (14), that ε_h and θ_h tend to zero uniformly in time ($t\in[0,T]$). In the same way, if $(u,\lambda)\in\mathcal{C}^3(0,T;X)\times\mathcal{C}^3(0,T;M)$ the same estimates hold for the second and third time derivatives of the errors. In particular

$$\left\{\begin{array}{l} \exists\,\sigma, \text{ independent of } h \text{ such that if } k=2,3,\ \forall t\ge 0 \\ \left\|\dfrac{d^k\epsilon_h}{dt^k}\right\|_X \le \sigma\left\{\inf_{(v_h\in X_h)}\left\|\dfrac{d^k u(t)}{dt^k}-v_h\right\|_X + \inf_{(\mu_h\in M_h)}\left\|\dfrac{d^k\lambda(t)}{dt^k}-\mu_h\right\|_M\right\}. \end{array}\right. \tag{32}$$

Let us assume that

$$\left\{\begin{array}{lll} u_h(0) = & \Pi_h u(0) \\ \\ \dfrac{du_h}{dt}(0) = & \Pi_h\dfrac{du}{dt}(0) \end{array}\right. \tag{33}$$

(i.e. we impose no error at time $t=0$ to simplify), then with appropriate energy estimates we obtain (see Appendix 1)

$$\left\{\begin{array}{l} \|\eta_h(t)\|_X \le (\dfrac{t^2}{2}+t)\sup_{[0,t]}\left|\dfrac{d^2\varepsilon_h}{dt^2}\right| \\ \\ \|\tau_h(t)\|_M \le \dfrac{1}{C'}\left(M(\dfrac{t^2}{2}+t)+1\right)\sup_{s\in[0,t]}\left|\dfrac{d^2\varepsilon_h}{dt^2}\right| + t\sup_{s\in[0,t]}\left|\dfrac{d^3\varepsilon_h}{dt^3}\right|, \end{array}\right. \tag{34}$$

where M is the continuity constant of the bilinear form $a(.,.)$

$$a(u,v) \leq M\|u\|_X\|v\|_X \quad \forall (u,v) \in X \times X, \tag{35}$$

and C' is the constant for the inf-sup condition. In conclusion, all the quantities $(\varepsilon_h(t),\theta_h(t),\eta_h(t),\tau_h(t))$ go to zero when h vanishes, uniformly for t in any bounded interval, as soon as the uniform discrete inf-sup condition is supposed. This implies that the error between the exact solution of problem (4) and the approximate solution of the semidiscrete problem (13) converges to zero with respect to h.

2.5 Stability

In this section, the stability of the numerical scheme is studied. The remarkable result is that our new scheme is stable under exactly the same condition as in the case without obstacle. Indeed, we define the discrete energy

$$E_h^{n+1/2} = \frac{1}{2}\|\frac{u_h^{n+1}-u_h^n}{\Delta t}\|^2 + a(u_h^{n+1},u_h^n). \tag{36}$$

Remark that scheme (17) is the "matrix form" of the following variational scheme

$$\begin{cases} (\dfrac{u_h^{n+1}-2u_h^n+u_h^{n-1}}{\Delta t^2}, v_h) + a(u_h^n, v_h) = b(v_h, \lambda_h^n) & \forall v_h \in X_h \\ b(u_h^n, \mu_h) = 0 & \forall \mu_h \in M_h, \end{cases} \tag{37}$$

Taking $v_h = \dfrac{u_h^{n+1}-u_h^{n-1}}{2\Delta t}$, we obtain

$$\frac{E_h^{n+1/2}-E_h^{n-1/2}}{\Delta t} + b(\frac{u_h^{n+1}-u_h^{n-1}}{2\Delta t}, \lambda_h) = 0. \tag{38}$$

Then if we take $\mu_h = \lambda_h^{n-1}$ (resp $\mu_h = \lambda_h^{n+1}$), we see that $b(u_h^n, \lambda_h^{n-1}) = 0$ (resp $b(u_h^n, \lambda_h^{n+1}) = 0$) for all n. Therefore $b(\dfrac{u_h^{n+1}-u_h^{n-1}}{2\Delta t}, \lambda_h) = 0$. So the discrete

energy $E_h^{n+1/2}$ is conserved.
Rewriting (36) as

$$\begin{aligned} E_h^{n+1/2} = \; & \frac{1}{2}\left\| \frac{u_h^{n+1}-u_h^n}{\Delta t}\right\|_X^2 \\ & -a(\frac{u_h^{n+1}-u_h^n}{2},\frac{u_h^{n+1}-u_h^n}{2}) + a(\frac{u_h^{n+1}+u_h^n}{2},\frac{u_h^{n+1}+u_h^n}{2}), \end{aligned} \tag{39}$$

the discrete energy $E_h^{n+1/2}$ is a positive quadratic form in u_h^n, u_h^{n+1} as soon as

$$\|v_h\|^2 - \frac{(\Delta t)^2}{4} a(v_h, v_h) > 0 \quad \forall v_h \in X_h \tag{40}$$

In this case, there is a conservation of a discrete energy and the scheme is L^2 stable. Condition (40) is nothing else than the usual CFL condition, which expresses that the time step Δt must satisfy

$$\frac{\Delta t}{h} < \alpha_{CFL} \tag{41}$$

where α_{CFL} is the stability threshold defined by

$$\alpha_{CFL}^2 = \sup_{u \in X_h} \frac{h^2 a(u,u)}{4 \, \|u\|_X^2}. \tag{42}$$

3 Fictitious domain solution for the Maxwell equations

3.1 Generalities

Here, we wish to deal with the scattering of an electromagnetic wave by a perfect conductor denoted by $\mathcal{O}$ ($\mathcal{O} \subset \mathbf{R}^d$ *with* $d = 2$ *or* $d = 3$). We reuse the same abstract formalism as in section 2. Let us first rewrite the Maxwell equations in term of the only electric field. The field satisfies the equations

$$\begin{cases} \dfrac{\partial^2 \vec{E}}{\partial t^2} + curl(curl\vec{E}) = 0 & \text{in } \mathbf{R}^d \backslash \mathcal{O} \\ \vec{n} \wedge (\vec{E} \wedge \vec{n}) = 0 & \text{on } \gamma \end{cases} \tag{43}$$

A Dirichlet condition or an absorbing boundary condition is assumed on the exterior boundary of the rectangular computation domain. So we look for the solution in the bounded domain Ω. The problem can still be written in the abstract form of (4) with the following identifications:

$$\begin{cases} u = \vec{E} \text{ is the electric field} \\ v = \vec{F} \text{ is the associated test function} \\ X = H(curl, C) \\ M = H^{-1/2}(div_\gamma, \gamma) \text{ if } d = 3 \text{ and } M = H_t^{1/2}(\gamma) \text{ if } d = 2 \\ (u, v) = \int_C uv\, dx \\ a(u, v) = \int_C curl(u) curl(v)\, dx \; b(u, \lambda) = \int_\gamma \vec{n} \wedge (\vec{E} \wedge \vec{n}).\lambda\, d\gamma \end{cases} \tag{44}$$

where $H^{-1/2}(div_\gamma, \gamma) = \left\{ v/v \in H_t^{-1/2}(\gamma), div_\gamma(v) \in H_t^{-1/2}(\gamma) \right\}$ and where $H_t^{-1/2} = \left\{ v/v \in H^{-1/2}(\gamma)/\langle v, \phi \rangle \forall \phi \in H^{1/2}(\gamma)/\phi \wedge n = 0 \right\}$(see [18] for more details) and $div_\gamma(v)$ is the tangential divergence on γ.

Physically, it is interesting to notice that the Lagrange multiplier represents the derivative in time of a surface current localized on the perfect conductor. In the following, we shall discuss the finite element approximation of problem (43)-(44).

3.2 Finite element approximation

3.2.1 Elements of X_h:

In order to take advantage of the fictitious domain method, we use regular grids for discretizing the domain C. In the 2D (resp 3D) case, we use squares (resp cubes). We consider for simplicity the lowest order Nédelec elements of the space $H(curl)$[22]. The degrees of freedom of such elements are the values

of the tangential component at the middle of the edges. A corresponding set of basis functions is obtained by associating to each edge the function whose tangential component is equal to 1 on that edge and equal to zero on the others.
The electric field is equal to

$$\vec{E} = \sum_{k=1}^{p} E_k \vec{v_k}, \tag{45}$$

where p is the number of degrees of freedom in the space H(curl) ($p = 2n_x\ n_y + n_x + n_y$ in the two dimensional case and $p = 3n_x\ n_y\ n_z + 3n_x\ n_y + 3n_x\ n_z + 3n_y\ n_z + 2n_y + 2n_z + 2n_x$ in the three dimensional case)

3.2.2 Elements of M_h:

In the 2D case, the Lagrange multiplier belongs to $H_t^{1/2}(\gamma)$. We can approximate the boundary γ by segments and choose the P1 elements for the approximation of the Lagrange multiplier. In the 3D case, the Lagrange multiplier belongs to $H^{-1/2}(div_\gamma, \gamma)$. The boundary which is now a surface, can be approximated by triangles and we can choose the lowest order Raviart-Thomas elements for M_h [13]. The degrees of freedom are the values of the normal components at the middle of the edges.
The multiplier can be written

$$\vec{\lambda} = \sum_{k=1}^{q} \lambda_k \vec{w_k} \tag{46}$$

where q is the number of degrees of freedom.

3.2.3 The discrete variational problem:

The problem can be now rewritten in the abstract form of (16). If we look for the solution in the form (45) and (46), we have

$$\begin{cases} \dfrac{d^2}{dt^2}\displaystyle\sum_{k=1}^{p} E_k \int_C \vec{v_k}\vec{v_i}\,dx + \sum_{k=1}^{p} E_k \int_C curl(\vec{v_k})curl(\vec{v_i})\,dx & \\ \qquad = \displaystyle\sum_{k=1}^{q} \lambda_k \int_\gamma \vec{w_k}\vec{v_i}\,dx & i = 1,\ldots,p \\ \displaystyle\sum_{k=1}^{p} E_k \int_\gamma \vec{w_j}\vec{v_k}\,dx = 0 & j = 1,\ldots,q \end{cases} \tag{47}$$

The $p \times p$ mass matrix is defined by

$$M_h(l,k) = \int_C \vec{v_l}\vec{v_k}\,dx \tag{48}$$

The $p \times p$ stiffness matrix is :

$$A_h(l,k) = \int_C curl(\vec{v_l})curl(\vec{v_k})\,dx. \tag{49}$$

The $p \times q$ "boundary matrix " is defined by

$$B_h(l,k) = \int_\gamma \vec{v_k}\vec{w_l}\,dx. \tag{50}$$

3.2.4 Time discretization

We have used the standard finite difference scheme for the time derivatives. After mass lumping, the problem to be solved is

$$\begin{cases} E_h^{n+1} - 2E_h^n + E_h^{n-1} = -\Delta t^2 M_h^{-1} A_h E_h^n + \Delta t^2 M_h^{-1} B_h \Lambda_h^n & (1) \\ B_h^t E_h^n = 0, & (2) \end{cases} \tag{51}$$

On a regular mesh, the electric field at time $n \times \Delta t$ can be split in two parts

$$\vec{E}(n \times \Delta t) = \sum_{i,j} E^n_{i+\frac{1}{2},j}\vec{x} + \sum_{i,j} E^n_{i,j+\frac{1}{2}}\vec{y} \tag{52}$$

where $E^n_{i+\frac{1}{2},j}$ denotes the x-component of the electric field at time $n \times \Delta t$ and at point $((i+\frac{1}{2})\, l_x, j\, l_y)$ (i.e at a point located at the middle of an horizontal wedge) and $E^n_{i,j+\frac{1}{2}}$ is defined similarly. Without the obstacle, the scheme is written as

$$\left\{\begin{array}{l} E^{n+1}_{i+\frac{1}{2},j} = 2E^n_{i+\frac{1}{2},j} - E^{n-1}_{i+\frac{1}{2},j} \\ \qquad +\dfrac{\Delta t^2}{l_y^2}(-E^n_{i+\frac{1}{2},j+1} + 2E^n_{i+\frac{1}{2},j} - E^n_{i+\frac{1}{2},j-1}) \\ \qquad +\dfrac{\Delta t^2}{l_x l_y}(E^n_{i,j-\frac{1}{2}} - E^n_{i+1,j-\frac{1}{2}} - E^n_{i+1,j+\frac{1}{2}} - E^n_{i,j+\frac{1}{2}}) \quad i = 1,\ldots,p \\ \\ E^{n+1}_{i,j+\frac{1}{2}} = 2E^n_{i,j+\frac{1}{2}} - E^{n-1}_{i,j+\frac{1}{2}} \\ \qquad +\dfrac{\Delta t^2}{l_x^2}(-E^n_{i+1,j+\frac{1}{2}} + 2E^n_{i,j+\frac{1}{2}} - E^n_{i-1,j+\frac{1}{2}}) \\ \qquad +\dfrac{\Delta t^2}{l_x l_y}(E^n_{i-\frac{1}{2},j} - E^n_{i-\frac{1}{2},j+1} - E^n_{i+\frac{1}{2},j+1} - E^n_{i+\frac{1}{2},j}) \quad j = 1,\ldots,q \end{array}\right. \tag{53}$$

One of the important property of these scheme is that it can be reinterpreted in the framework of the finite-difference time-domain method or FDTD, [24]. Let us consider the system

$$\left\{\begin{array}{l} \dfrac{H^{n+1/2} - H^{n-1/2}}{\Delta t} + R_h E^n = 0 \\ \dfrac{E^{n+1} - E^n}{\Delta t} - R_h^t H^{n+1/2} = \dfrac{1}{h^2} B_h \lambda^{n+1/2} \\ B_h^t E^n = 0 \end{array}\right. \tag{54}$$

where R_h stands for the discrete curl operator constructed on staggered grids of steps h and R_h^t for its transpose. If we forget about the term in $\lambda^{n+1/2}$, the two first equations in (54) are nothing else than the classical Yee scheme for

the FDTD, [23]. From (54), we deduce

$$\begin{cases} \dfrac{1}{\Delta t}\left(\dfrac{E^{n+1}-E^n}{\Delta t}-\dfrac{E^n-E^{n-1}}{\Delta t}\right)-R_h^t\left(\dfrac{H^{n+1/2}-H^{n-1/2}}{\Delta t}\right) \\ \qquad =\dfrac{1}{h^2}B_h\left(\dfrac{\lambda^{n+1/2}-\lambda^{n-1/2}}{\Delta t}\right) \end{cases}$$

or

$$h^2\,\frac{E^{n+1}-2E^n+E^{n-1}}{\Delta t^2}+h^2R_h^tR_hE^n=B_h\Lambda_h^n$$

where we have set

$$\frac{\lambda^{n+1/2}-\lambda^{n-1/2}}{\Delta t}=\Lambda^n$$

If we remark that the assembly of the mass matrix and stiffness matrices for the lowest order Nédelec's elements calculated with mass lumping and for isotropic meshes (i.e. $l_x=l_y=h$) gives

$$M_h=h^2Id,\quad A_h=h^2R_h^tR_h$$

we finally obtain the equivalence between system (51) and (54).

In this context, the scheme is solved according to

$$\begin{cases} H^{n+1/2}=H^{n-1/2}-\Delta tR_hE^n \\ E_{FDTD}^{n+1}=E^n+\Delta tR_h^tH^{n+1/2} \\ \Lambda^n=\left(B_h^t\dfrac{1}{h^2}B_h^t\right)^{-1}B_h^tE_{FDTD}^{n+1} \\ E^{n+1}=E_{FDTD}^{n+1}-\dfrac{\Delta t}{h^2}B_h^t\Lambda^n \end{cases} \tag{55}$$

In system (55), the obstacle is incorporated inside the scheme by modifying the classical two-steps FDTD. At first, the surfacic current Λ^n is determined by solving the small linear system with matrix $B_hB_h^t$ then, the electric field is modified to take into account this current. This remark is important as most of the usual codes for transient electromagnetics are based on FDTD. What we propose here is to include diffraction effects by simply adding two steps in the classical calculation.

3.2.5 Absorbing boundaries

It has been previously seen that the scheme is equivalent to the usual Yee scheme at points localized far away the obstacle. We can then reuse the standart techniques to implement appropriate numerical absorbing conditions. For simplicity, the Joly-Mercier's conditions [17] have been retained. Let us recall that these conditions imply first order derivative operators for second order accuracy (i.e an accuracy equivalent to the one of Mur conditions [21]). There are obtained via a standart discretization of the equations

$$\begin{cases} \dfrac{\partial E_y}{\partial t} - \dfrac{\partial E_y}{\partial x} + \dfrac{1}{2}\dfrac{\partial E_x}{\partial y} = 0 \quad \text{at the west boundary} \quad (1) \\ \dfrac{\partial E_y}{\partial t} + \dfrac{\partial E_y}{\partial x} - \dfrac{1}{2}\dfrac{\partial E_x}{\partial y} = 0 \quad \text{at the east boundary} \quad (2). \end{cases} \tag{56}$$

The boundary conditions at the south and the north sides are obtained similarly , interchanging x and y. At the corner, special conditions [4] obtained by compatibility have been used. For instance at the Northwest corner, we have to discretize the corner condition

$$\begin{cases} \dfrac{\partial E_y}{\partial t} - \dfrac{\partial E_y}{\partial x} + \dfrac{1}{2}\dfrac{\partial E_x}{\partial y} = 0 \\ \dfrac{\partial E_x}{\partial t} - \dfrac{\partial E_x}{\partial y} + \dfrac{1}{2}\dfrac{\partial E_y}{\partial x} = 0. \end{cases} \tag{57}$$

Note that the choice of the conditions at the boundary is crucial to bound the computation domain but is not related with the implementation of the fictitious domain method. In the next part, numerical results are presented with a Dirichlet condition on the outer boundary of the obstacle or with a second order absorbing boundary condition.

4 Numerical experiments

4.1 Generalities

We want to show how the fictitious domain method is able to solve time-dependent Maxwell equations and also to demonstrate that the solution obtai-

ned from the fictitious domain method is better in terms of accuracy than the solution obtained by approximating the exact boundary by a staircase discrete boundary.

The test problems to be discussed concern the solution of the problem described in section 3.1, 3.2. We perform a Cholesky factorization of the matrix $B_h^t M_h^{-1} B_h$ before starting the time iterations.

4.2 Computation of the matrix B

The matrix B can be seen as a discrete trace operator from M_h to X_h and can be written as a line integral

$$B(i,j) = \int_\gamma \vec{v_j}\vec{w_i}\, ds \tag{58}$$

Note that for more simplicity, we have chosen to take the P^0 elements basis for the discretization of the space Y. In theory, this choice does not fit the general framework described in section 2 and 3 since piecewise constant functions do not belong to $H^{1/2}$. However, as we choose a subspace of L^2 for approximating both $H^{1/2}$ and $H^{-1/2}$ the bilinear form $b(v,\lambda)$ defined by (58) still takes sense as an integral in the discrete case which justifies our choice.

The computation of the integral (58) can be done in two manners:

- an exact computation which requires the intersection between the volume and surface meshes X_h and Y_h and then the integration of quadratic functions,
- an approximate computation based on a Riemann sum:

$$B(i,j) = \sum_{k=1}^{N_{riem}} \lambda_j(s_k) w_i(s_k) \Delta s \tag{59}$$

where s_k are the integration points, separated by Δs and N_{Riem} is the number of integration points.

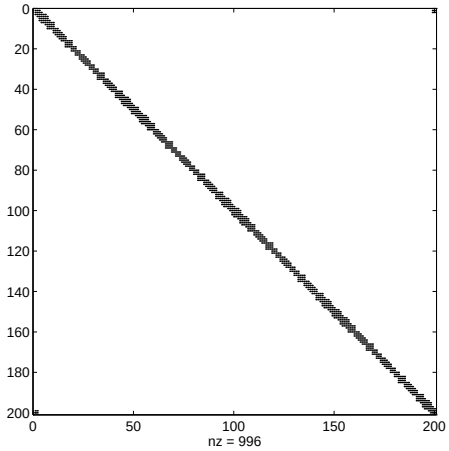

Fig 5: *Example of the sparsity pattern of the matrix Q*

The numerical implementation of the Riemann method is very easy and can be used to test the first method. But its computational time increases when N_{Riem} increases.

We show in Fig 5 the sparsity pattern of the matrix $Q = B_h^t M_h^{-1} B_h$ when the obstacle is a disk and when h_s is equal to h_v. The maximum eigenvalue of the matrix Q may be computed.

The figure 6 shows the difference of the maximum eigenvalues obtained by the two methods divided by the maximum eigenvalue computed by the first method when the obstacle is an inclined plane. We have noticed that this curve does not change drastically with the geometry of the obstacle. When the number of integration points is greater than one hundred, the relative error is less than one per cent. We have also studied the matrix condition number. It does not change with the number of integration points in the case of the Riemann method. But it is very dependent of the quotient of the step sizes of the two meshes (see Fig 7).

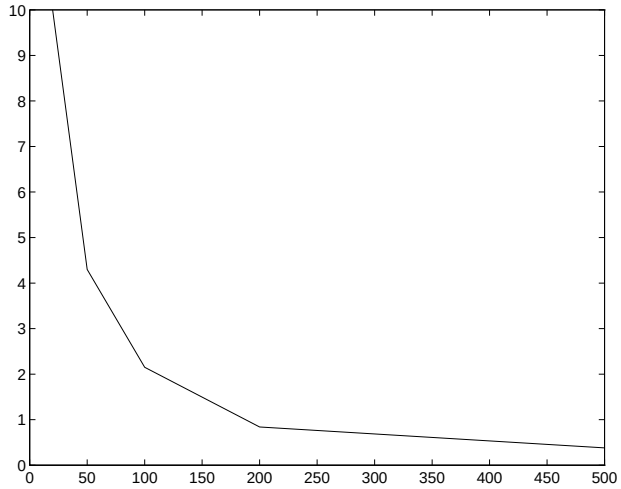

Fig 6: *Relative error on the maximum eigenvalue of Q versus the number of integration points*

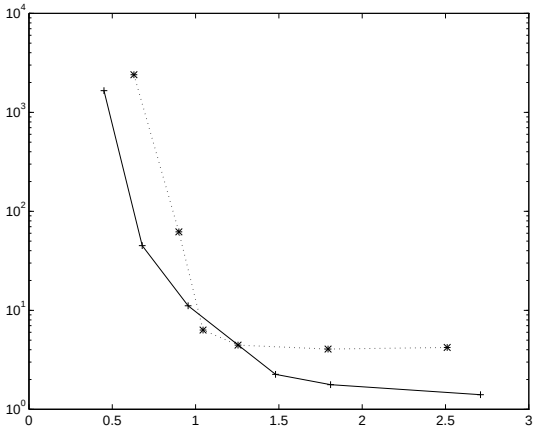

Fig 7: *Matrix condition number versus h_s/h_v (- :when the obstacle is a inclined plane and ...: when the obstacle is a disk)*

4.3 A first test: reflection on a plane

A first experience leading to interesting conclusions deals with the reflection on a plane of a wave produced by a point source in 2D

$$S(p,t) = g(t)\ curl\,(\,\delta(p-p_s)\cdot\vec{e}_3\,)\,, \qquad g(t) = \frac{d}{dt}\left(\exp^{-(t/t^0)^2}\right), \tag{60}$$

where $\vec{e}_3$ is the vector perpendicular to the computational plane. t^0 is equal to 0.145 s and p_s is a point located at 0.68 m from the reflecting plane. The time function is depicted in figure 8. Mass lumped edge elements on a regular square grid are used for the discretization of space X [20].

We consider two cases:

- Reference case: the plane is vertical.
- Test case: the plane is inclined at an angle θ with the vertical plane

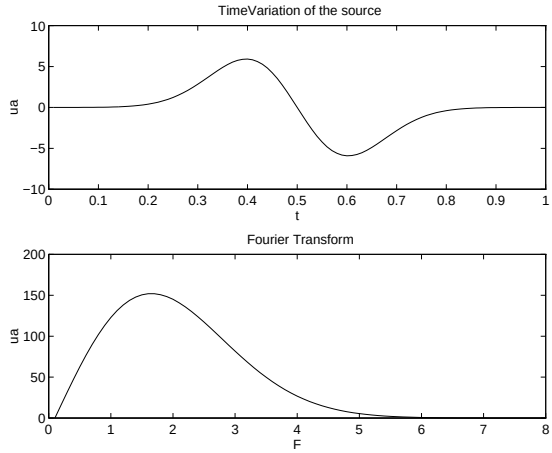

Fig 8: *Time evolution of the source and its Fourier transform*

In case A, the object is discretized on the regular grid mesh. The finite difference method and the fictitious domain method give rigorously the same results. On the contrary, in case B, the object does not coincide with the regular grids. The finite difference has the disadvantage to produce numerical diffractions. We want to show how the fictitious domain method is able to produce much closer results than those obtained in case A with the usual finite difference approach. To achieve this, we compare the snapshots of propagation for these two cases and the trace recording for various situations.

Figure 9-10 compare two snapshots taken at the same instant and computed by the fictitious domain method for the two positions of the reflecting plane. We can see the good agreement of the two pictures. Figure 11 and 12 are more interesting since they plot to the area of time corresponding of the arrival of reflected waves. They clearly show the gain in accuracy due to the fictitious domain method when one discretizes with 10 points per shortest wavelength ($\lambda^- = 0.2 \ \Rightarrow h_v = 0.02$). Of course (see Fig 13 corresponding to the same comparison but with $h_v = 0.01$), when the step size goes to zero, all solutions converge to the true solution. Figure 14-15 shows that the quality of the results is not affected when one increases the step on the boundary for a fixed space increment. This is interesting since the computational cost due to the auxiliary unknown determination and linked to the size of the matrix Q is decreased.

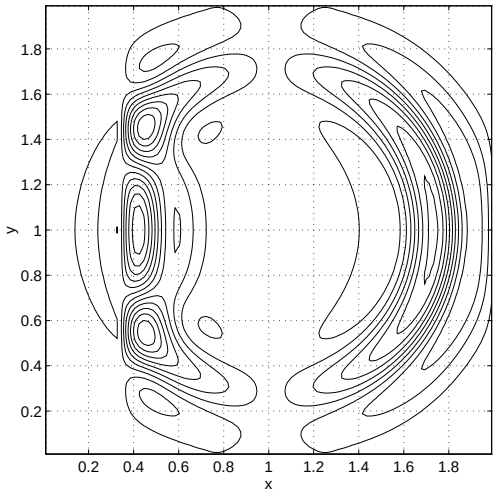

Fig 9: *Snapshot at t = 1.26 s. of the tangential component of the electric field with a vertical reflecting plane*

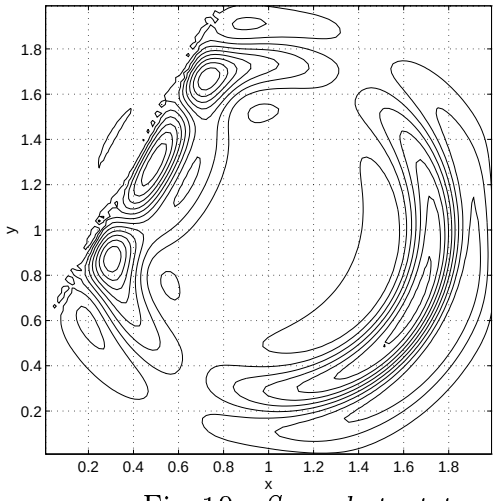

Fig 10: *Snapshot at t = 1.26 s. of the tangential component of the electric field when the plane is inclined at an angle of 28 degree*

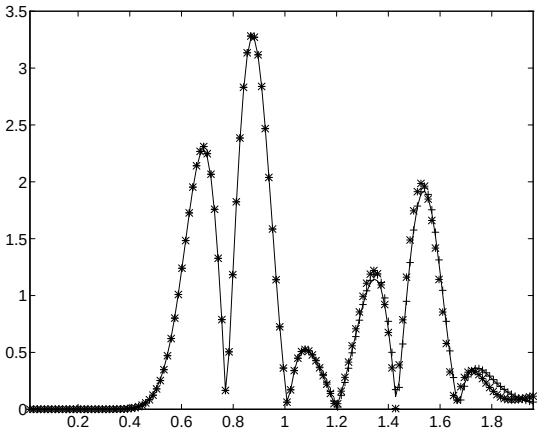

Fig 11: *Ponctual trace-recording of the modulus of the electric field (- :reference case, +: test case, *: stair case) (h_v=h_s=0.02)*

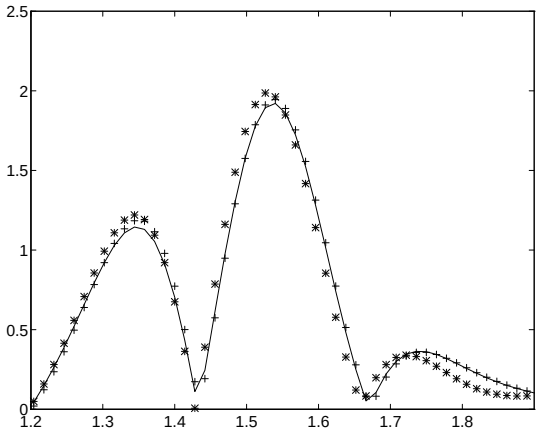

Fig 12: *Zoom of Figure 11*

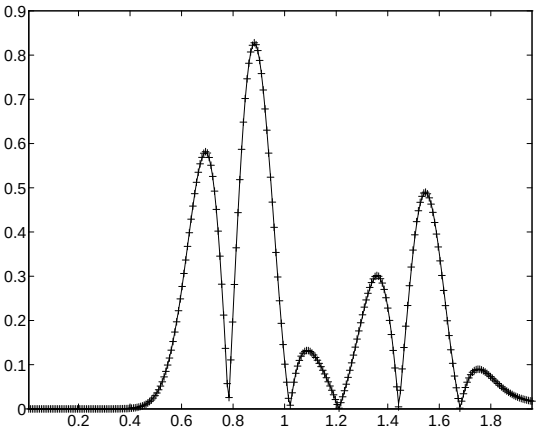

Fig 13: *Same as figure 11 but with* $h_v = h_s$*=0.01*

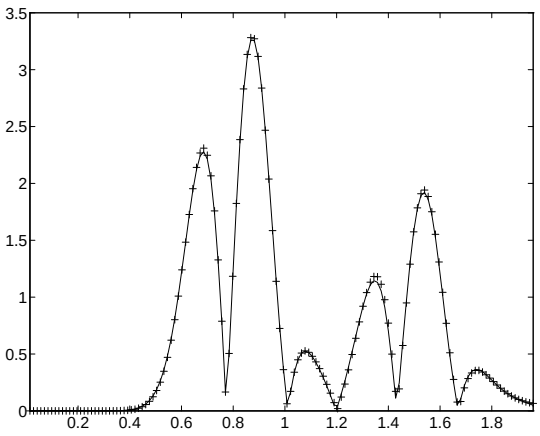

Fig 14: *Same as figure 11 but with* h_v *= 0.02,* $h_s = 0.03$

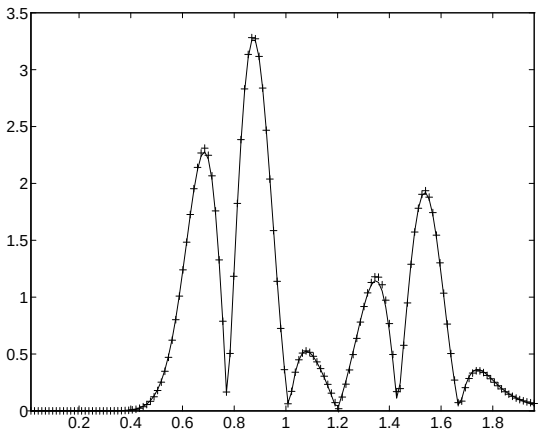

Fig 15: *Same as figure 11 but with* $h_v = 0.02$*,* $h_s = 0.04$

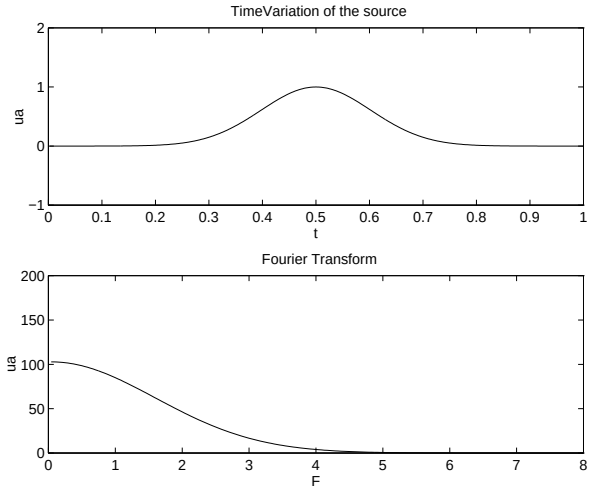

Fig 16: *Time evolution of the source and its Fourier transform*

4.4 A second test: a wedge

We have computed the electric field reflected by a dihedral (see Fig 17) when it is illuminated by a harmonic wave. The incident electric field propagates in the x-direction and has only a component on the y-axis

$$\vec{E_{inc}}(t,x,y) = \frac{dg(t)}{dt}\,\delta(x-x_s)\,\vec{e_y} \qquad ; g(t) = \left(\exp^{-(t/t^0)^2}\right), \tag{61}$$

where x_s is an abscissa located at 0.2 from the wedge. Figures (18-19) give the snapshots of the y-component of the electric field at different times.

Figure 20 shows the trace-recording of the electric field when the number of points by wavelength is increased. All the curves are close to each other. So a discretization with 10 points per wavelength seems to be adequate.
Figures(21-22-23) compare the amplitude of the electric field obtained with the staircase approximation of the boundary and for various number of points per wavelength (10,20,40) with the result obtained by the fictitious method with ten points per wavelength. All the curves obtained with the FDTD method present oscillations due to the numerical diffractions because the obstacle does not fit the regular mesh X_h. We can also remark that these curves tend to fit the curve obtained from the fictitious domain method when the number of

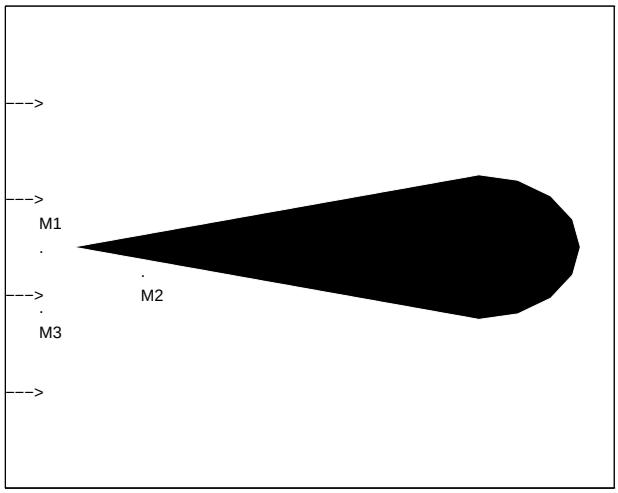

Fig 17: *Configuration of the geometry of the scattering problem (M1:(0.3,1);M2(0.6,0.9),M3(0.3,0.75))*

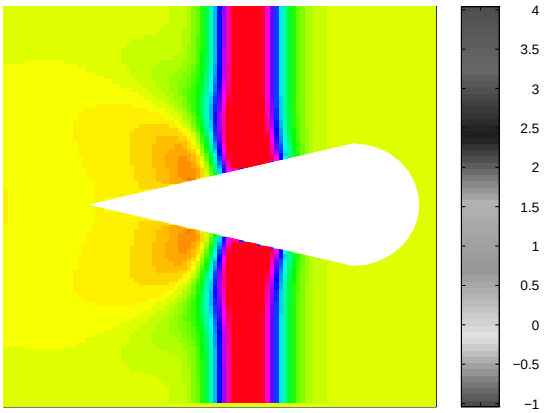

Fig 18: *Snapshot of the y-component of the electric field at time* $t = 0.13s$

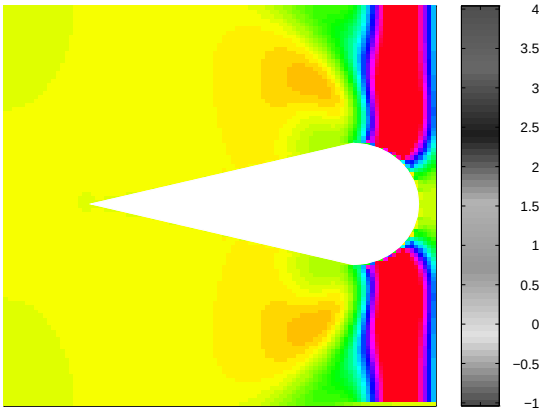

Fig 19: *Same as Fig. 18 but at time* $t = 27s$

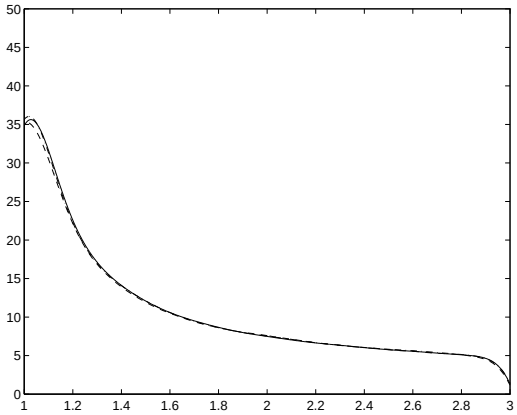

Fig 20: *Ponctual trace-recording of the modulus of the electric field at M1 obtained by the fictitious method for various values of the number of points per wavelength nw (−:nw = 10, -. :nw = 20,-:nw = 40)*

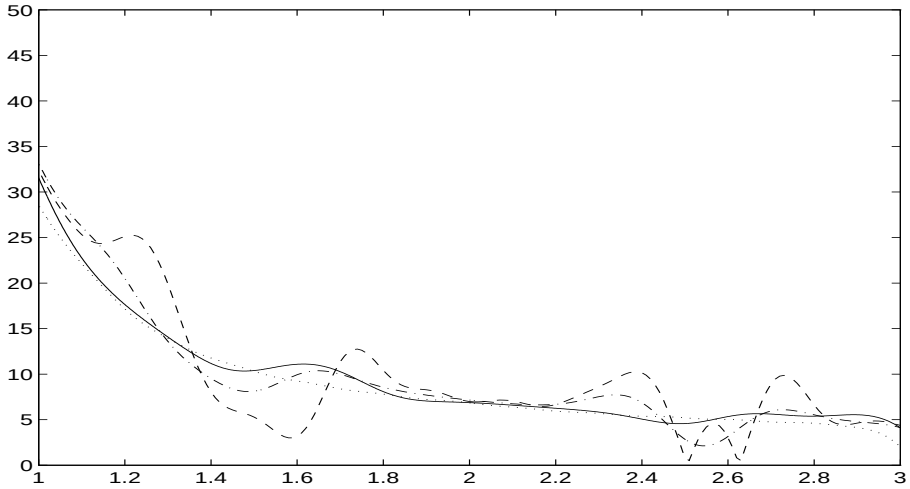

Fig 21: *Ponctual trace-recording of the modulus of the electric field at M1 obtained by (...:fictitious method (nw = 10), - - :FDTD method (nw = 10), -.:FDTD (nw = 20),-:FDTD (nw = 40))*

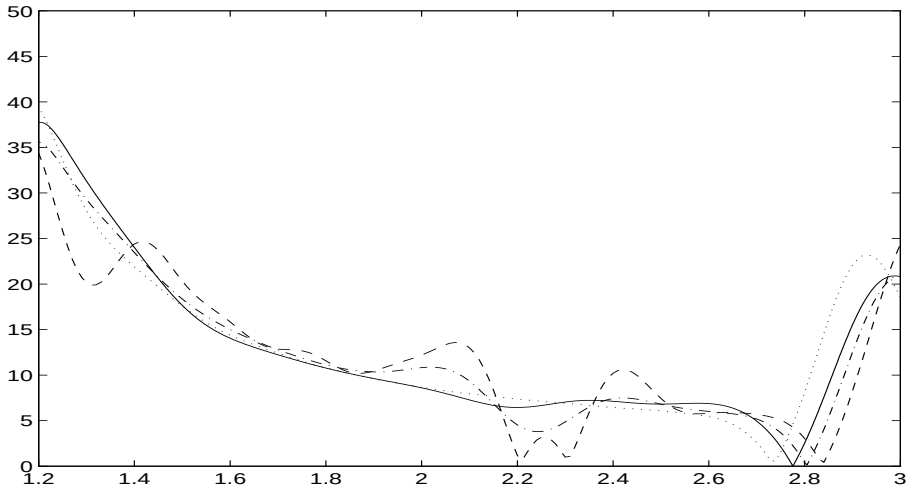

Fig 22: *Same as figure 11 at M2 (0.6, 0.9)*

points per wavelength is increased. In conclusion, the fictitious domain method is superior in one hand in terms in accuracy than the FDTD method and in the other hand in terms of the required space memory.

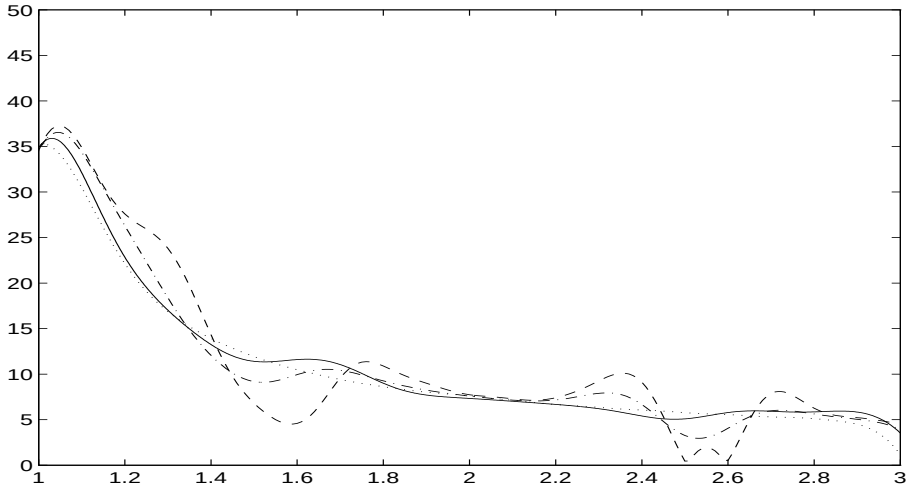

Fig 23: *Same as figure 11 at M3 (0.3, 0.75)*

5 Conclusion

A fictitious domain method has been introduced for unsteady scattering problems. This method consists in extending the solution inside the object and in introducing an auxiliary variable defined on the boundary. Its main advantage is to permit the use of uniform meshes for the solution. An additional cost is due to the computation of the auxiliary variable. This also imposes a non really restrictive compatibility relation between the boundary mesh for the auxiliary unknown and the uniform mesh for the solution. In this paper, we have applied this method for solving time dependent Maxwell's equations. We have tested this algorithm in the 2D case for the scattering on a perfect conductor plane. Numerical results show the superiority (in terms of accuracy and memory space) of the fictitious method over the FDTD method. This method may be also extended for solving three dimensional problems where geometrical difficulties appear due to the intersection of the two meshes ([9]). This fictitious method is applied for solving problems with a Dirichlet condition on the boundary of the obstacle. Moreover, it may be used also for problems with a Neumann condition on the obstacle without any difficulty. But some investigation must be necessary to treat other boundary conditions as an impedance condition. This will be the subject of a future work.

6 Acknowledgement

We would like to thank Pr. R. Glowinski for helpful comments and suggestions and also S. Garcés for discussions about numerical and theoretical points.

References

[1] G.P. Astrakmantev, *Methods of fictitious domains for a second order elliptic equation with natural boundary conditions*, U.S.S.R Computational Math.and Math. Phys.,18(1978),pp. 114-221.

[2] C. Atamian,R. Glowinski,J. Periaux,H. Steve and G. Terrason, *Control approach to fictitious domain in electro-magnetism*, Conference sur l'approximation et les methodes numeriques pour la resolution des equations de Maxwell,Hotel Pullmann, Paris ,(1989).

[3] C. Atamian and P. Joly,*Une analyse de la methode des domaines fictifs pour le probleme de Helmholtz exterieur*,Technical report,I.N.R.I.A.,rapport interne 1378,(1991).

[4] A. Bamberger, P. Joly and J. Roberts, *second order absorbing boundary conditions for the wave equation; a solution for the corner problem* SIAMJ. on Num. Anal.,17(1990),pp. 323-352

[5] A. Bendali, *Approximation par elements finis de surface de problemes de diffraction des ondes electro-magnetiques*,PHD thesis, Paris VI(1984)

[6] F. Brezzi,*On the existence uniqueness and approximation of saddle-point problems arising from Lagrangian multipliers*, Revue Francaise d'Automatique, Informatique et Rcherche Opérationnelle,R-2,pp. 129-151,(1974)

[7] G.Cohen,P.Joly and N. Tordjman,*méthodes numériques d'ordre élevé pour les ondes en régime transitoire*, Ecole INRIA des ondes,(1994).

[8] F. Collino,*Conditions aux limites absorbantes d'ordre élevé pour des modèles de propagation d'ondes dans des domaines rectangulaires*,Technical report,I.N.R.I.A.,rapport interne 1991 (1993).

[9] F. Collino et all,*Fictitious domain method for unsteady problems: application to electromagnetic scattering* , ICEAA, Torino,(1995)

[10] T.Dupontℓ^2-*estimate for Galerkin methods for second order hyperbolic equations*, SIAM J. Numer. Anal., Vol. 10,No 5, October 1973

[11] B. Engquist and A. Majda,*Absorbing boundary conditions for the numerical simulation of waves*,Comm. Pure. Appl. Math.,32(1979),pp. 313-357.

[12] S.A Finogenov and Y.A. Kuznetsov,*Two stage fictitious components methods for solving the Dirichlet boundary value problem*,Sov. J. Num. Anal. Math. Modelling,3(1988),pp 301-323

[13] S. Garcés ,*Application des méthodes de domaines fictifs à la modélisation des structures rayonnantes tridimensionnelles* , PHD thesis in preparation

[14] V.Girault and R. Glowinski,*Error analysis of a fictitious domain method applied to a Dirichlet problem* , to appear (1994)

[15] R. Glowinski and T.W. Pan and J. Periaux,*A fictitious domain method for Dirichlet problem and applications*, Comp. Meth. in Appl. Mech. and Eng., pp 283-303, 1994

[16] R. Glowinski and T.W. Pan and J. Periaux,*A fictitious domain method for external incompressible viscous flow modeled by Navier-Stokes equations*, Comp. Meth. in Appl. Mech. and Eng., pp 283-303, 1994

[17] P. Joly and B. Mercier,*Une nouvelle condition aux limites transparentes d'ordre 2 pour les equations de Maxwell en dimension 3*,Technical report,I.N.R.I.A.,rapport interne 1047(1989).

[18] R. Dautray and J.L LIons, Analyse mathèmatique et calcul numérique pour les sciences et techniques, Masson, Paris (1979)

[19] G.I Marchuk,Y.A Kuznetsov and A.M. Matsokin, *Fictitious domain and domain decomposition methods*,Sov. J. Num. Anal. Math. Modelling, 1(1986),pp. 3-35.

[20] P. Monk, *A mixed method for approximating Maxwell's equations* ,SIAM J. on Num. Anal. Math. Modelling, 28(1991),pp. 1610-1634.

[21] G. Mur, *Absorbing boundary conditions for the finite difference approximation of the time-domain electromagnetic field equations* ,IEEE Trans. Electromagn. Compat. 23(1981),pp. 377-382.

[22] J.C Nedelec, *Mixed finite elements in* $\mathbf{R}^3$,Num.Math.,142(1984),pp 79-85.

[23] K.S Yee, *Numerical solution of initial boundary value problems involving Maxwell's equations in isotropic media*,IEEE. on antennas and propagation,vol AP14(1966),pp 302-307.

[24] A.Taflove ,*Computational Electrodynamics, The Finite-Difference Time Domain method*,Artech House, London,(1995).

6.1 APPENDIX 1: About error estimates

The aim of this appendix is to demonstrate the inequalities (34) of subsection 2.4.

We start from the variationnal equalitie satisfied by $u(t)$ applied to a test function $v = v_h$ in X_h ;

$$\frac{d^2}{dt^2}(u, v_h) = -a(u, v_h) + b(v_h, \lambda) \quad \forall v_h \in X_h, \tag{62}$$

or, using $\epsilon_h(t) = \Pi_h u(t) - u(t)$,

$$\frac{d^2}{dt^2}(\Pi_h u, v_h) = -a(u, v_h) + b(v_h, \lambda) - \left(\frac{d^2\varepsilon_h}{dt^2}, v_h\right) \quad \forall v_h \in X_h. \tag{63}$$

The definition of the elliptic projector allows us to replace (u, λ) by $(\Pi_h u, \Pi_h \lambda)$, i.e.

$$\frac{d^2}{dt^2}(\Pi_h u, v_h) + a(\Pi_h u, v_h) - b(v_h, \Pi_h \lambda) = -\left(\frac{d^2\varepsilon_h}{dt^2}, v_h\right) \tag{64}$$

Otherwise, u_h verifies

$$\frac{d^2}{dt^2}(u_h, v_h) = -a(u_h, v_h) + b(v_h, \lambda_h) \quad \forall v_h \in X_h. \tag{65}$$

Subtracting (65) from (64), and using $\dfrac{d^2\eta_h}{dt^2} \in X$, (regularity of $u(t)$ and $u_h(t)$) we obtain

$$\left(\frac{d^2\eta_h}{dt^2}, v_h\right) + a(\eta_h, v_h) - b(v_h, \tau_h) = -\left(\frac{d^2\varepsilon_h}{dt^2}, v_h\right) \quad \forall v_h \in X_h. \tag{66}$$

Now, η_h is such that

$$b(\eta_h(t), \mu_h) = b(\Pi_h u - u, \mu_h) + b(u, \mu_h) - b(u_h, \mu_h) \quad \forall \mu_h \in M_h. \tag{67}$$

from which we deduce, using the properties of Π_h and the definition of u and u_h,

$$b(\eta_h(t), \mu_h) = b(\frac{d^k \eta_h(t)}{dt^k}, \mu_h) = 0 \quad \forall \mu_h \in M_h, \ k = 1, 2. \tag{68}$$

Let us set $v_h = \dfrac{d\eta_h}{dt}$ in (66), we obtain

$$\left\{ \begin{array}{l} \dfrac{d}{dt}\left(\dfrac{1}{2}E_h(t)\right) - b\left(\dfrac{d\eta_h}{dt}, \tau_h\right) = \left(\dfrac{d^2\varepsilon_h}{dt^2}, \dfrac{d\eta_h}{dt}\right) \\ E_h(t) = \left|\dfrac{d\eta_h}{dt}\right|^2 + a(\eta_h, \eta_h) \end{array} \right. \tag{69}$$

taking $k = 1,\ \mu_h = \tau_h(t)$ in (68), the b term vanishes and we get

$$\frac{1}{2}\frac{d}{dt}\left(E_h(t)\right) \leq \left|\frac{d^2\varepsilon_h}{dt^2}\right| \left|\frac{d\eta_h}{dt}\right| \Rightarrow \frac{d}{dt}E_h^{1/2} \leq \left|\frac{d^2\varepsilon_h}{dt^2}\right| \tag{70}$$

Using the fact

$$u_h(0) = \Pi_h u(0) \ \text{ and } \frac{du_h}{dt}(0) = \Pi_h \frac{du}{dt}(0), \tag{71}$$

we have

$$\begin{array}{l} \sqrt{a(\eta_h, \eta_h)} \ \text{ and } \ \left|\dfrac{d\eta_h}{dt}\right| \leq \displaystyle\int_0^t \frac{dE_h^{1/2}}{ds}(s)ds \ \leq t \sup_{[0,t]} \left|\frac{d^2\varepsilon_h}{dt^2}\right|. \\ |\eta_h(t)| \leq \displaystyle\int_0^t E_h^{1/2}(s)ds \leq \int_0^t \int_0^s \left|\frac{d^2\varepsilon_h}{dt^2}\right| dsdt \leq \frac{t^2}{2} \sup_{[0,t]} \left|\frac{d^2\varepsilon_h}{dt^2}\right| \end{array} \tag{72}$$

therefore

$$\|\eta_h\|_X = \sqrt{|\eta_h|^2 + a(\eta_h, \eta_h)} \leq (\frac{t^2}{2} + t) \sup_{[0,t]} \left|\frac{d^2\varepsilon_h}{dt^2}\right|. \tag{73}$$

We have obtained the inequality (34) for the error η_h. To get the second inequality, we start from the inf-sup condition

$$\|\tau_h(t)\|_M \leq \frac{1}{C'} \sup_{v_h \in X_h} \frac{b(v_h, \tau_h)}{\|v_h\|_X} \tag{74}$$

and we use both equation (66) and the continuity of the bilinear form a to get

$$\begin{array}{l} |b(v_h, \tau_h)| \leq \left|\left(\dfrac{d^2\eta_h(t)}{dt^2}, v_h\right)\right| + |a(\eta_h(t), v_h)| + \left|\left(\dfrac{d^2\varepsilon_h}{dt^2}, v_h\right)\right| \\ \qquad \leq M \|\eta_h\|_X \|v_h\|_X + \left(\left|\dfrac{d^2\eta_h}{dt^2}\right| + \left|\dfrac{d^2\varepsilon_h}{dt^2}\right|\right) |v_h| \quad \forall v_h \in X_h. \end{array} \tag{75}$$

Till now, we only have used the C^2 regularity of the solution. In order to bound the H-norm of $\dfrac{d^2\eta_h}{dt^2}$, we needs C^3. Indeed, in this case, all the previous calculations can be rewritten for the derivative of the functions. In particular, we have

$$\left|\frac{d^2\eta_h}{dt^2}\right| \leq t \sup_{[0,t]} \left|\frac{d^3\varepsilon_h}{dt^3}\right|.$$

Finally, combining the different results provides us

$$\begin{aligned} C' \left\|\tau_h(t)\right\|_M &\leq \left(M \left\|\eta_h\right\|_X + t \sup_{[0,t]} \left|\frac{d^3\varepsilon_h}{dt^3}\right| + \left|\frac{d^2\varepsilon_h}{dt^2}\right| \right) \\ &\leq \left(M(\frac{t^2}{2} + t) + 1 \right) \sup_{s\in[0,t]} \left|\frac{d^2\varepsilon_h}{dt^2}\right| + t \sup_{s\in[0,t]} \left|\frac{d^3\varepsilon_h}{dt^3}\right|, \end{aligned}$$

and the proof is achieved.

6.2 APPENDIX 2: A plane wave analysis of a 1-D problem

This section is devoted to a plane wave analysis of a simple problem : a 1-D wave equation with a boundary Dirichlet condition (see Fig 22). The interest of this case is essentially academic: we prove that the fictitious domain method gives rise to a better approximation than the staircase approximation. More

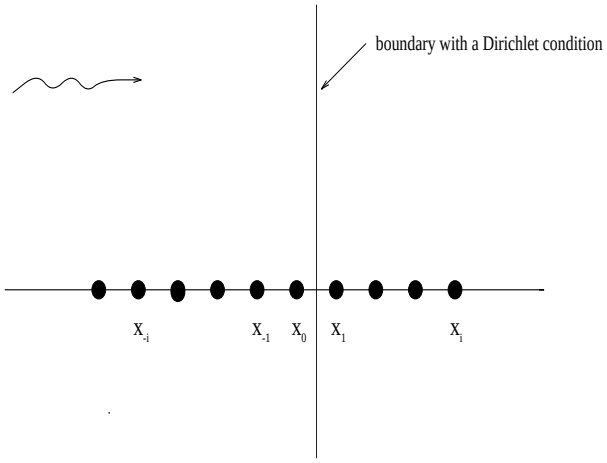

Fig 22: *Geometry of the problem*

precisely, we consider the problem

$$\begin{cases} \dfrac{\partial^2 u}{\partial t^2} - \dfrac{\partial^2 u}{\partial x^2} = 0, \quad x < x_\ell \\ u(x = x_\ell) = 0. \end{cases} \tag{76}$$

Let Δt and h the time and space steps, we assume the point x_ℓ to be closed to the point 0:

$$x_\ell = \ell h,\ 0 \leq \ell \leq \frac{1}{2}. \tag{77}$$

The classical space and time second order scheme for the staircase approximation is given by

$$\begin{cases} \dfrac{u_j^{n+1} - 2u_j^n - u_j^{n-1}}{\Delta t^2} - \dfrac{u_{j+1}^n - 2u_j^n + u_{j-1}^{n-1}}{h^2} = 0, \quad \forall j \leq -1 \\ u_0^n = 0. \end{cases} \tag{78}$$

In this case (staircase approximation), the point x_l has been shifted to the point 0.

On the other hand, it is not difficult to write the scheme obtained by the fictitious domain method

$$\begin{cases} \dfrac{u_j^{n+1} - 2u_j^n - u_j^{n-1}}{\Delta t^2} - \dfrac{u_{j+1}^n - 2u_j^n + u_{j-1}^{n-1}}{h^2} = \dfrac{\lambda^n}{h}\left((1-\ell)\delta_j^0 + \ell\delta_j^1\right) \quad \forall j \\ \ell u_1^n + (1-\ell)u_0^n = 0. \end{cases} \tag{79}$$

The problem has been extended to the whole space and a Lagrange multiplier λ has been added. Now, let us consider the plane wave solutions.
For the continuous problem (76), an incident plane wave gives rise to a reflected wave and the corresponding solution can be written

$$\begin{cases} u(x,t) = e^{i\omega t}\left(e^{-ik(x-x_\ell)} + Re^{ik(x-x_\ell)}\right), \quad x \leq x_\ell \\ \omega = k \quad \text{(dispersion relation)} \\ R = -1 \quad \text{(reflection coefficient)}. \end{cases} \tag{80}$$

For the staircase scheme (78), we obtain

$$\begin{cases} u_j^n = e^{i\omega n\Delta t}\left(e^{-ikh(j-\ell)} + Re^{ikh(j-\ell)}\right), \quad j \leq 0 \\ \dfrac{2}{\Delta t}\sin\left(\omega\dfrac{\Delta t}{2}\right) = \dfrac{2}{h}\sin\left(k\dfrac{h}{2}\right) \quad \text{(dispersion relation)} \\ R = -e^{2ikh\ell} \quad \text{(reflection coefficient)} \end{cases} \tag{81}$$

while for the fictitious domain scheme (79), the incident plane wave gives rise not only to a reflected wave but also to a transmitted wave (inside the fictitious

domain). More precisely, the solution we are looking for can be written

$$\begin{cases} u_j^n = e^{i\omega n\Delta t}\left(e^{-ikh(j-\ell)} + Re^{ikh(j-\ell)}\right), \quad j \le 0 \\ u_j^n = e^{i\omega n\Delta t} T e^{-ikh(j-\ell)}, \quad j \ge 1 \\ \lambda^n = e^{i\omega n\Delta t}\hat{\lambda} \\ \dfrac{2}{\Delta t}\sin\left(\omega\dfrac{\Delta t}{2}\right) = \dfrac{2}{h}\sin\left(k\dfrac{h}{2}\right) \quad \text{(dispersion relation).} \end{cases} \tag{82}$$

To find the 3 unknowns R, T and $\hat{\lambda}$ in (82), the equations of the scheme associated to the nodes $j = 0$ and $j = 1$ as well as the contraint equation are used. The following system is obtained

$$\begin{cases} z^\ell + R\,(1/z)^\ell - Tz^\ell = -\hat{\lambda}h\,\ell \\ T(1/z)^{(1-\ell)} - ((1/z)^{(1-\ell)} + R\,z^{(1-\ell)}) = -\hat{\lambda}h\,(1-\ell) \\ \ell T\,(1/z)^{(1-\ell)} + (1-\ell)(z^\ell + R\,(1/z)^\ell) = 0, \end{cases} \tag{83}$$

where z is given by

$$z = e^{ikh}. \tag{84}$$

Solving this system gives

$$\begin{cases} \hat{\lambda}h &= \dfrac{(z-z^{-1})(-\ell z^{\ell-1} - z^\ell + \ell z^\ell)z}{2\ell - 2\ell^2 + z - 2\ell z + 2\ell^2 z} \\ R &= -\dfrac{(2z^{2\ell-1}\ell - 2z^{2\ell-1}\ell^2 + z^{2\ell} - 2\ell z^{2\ell} + \ell^2 z^{2\ell} + z^{2\ell-2}\ell^2)z}{2\ell - 2\ell^2 + z - 2\ell z + 2\ell^2 z} \\ T &= \dfrac{\ell(1-\ell-z^2+\ell z^2)}{2\ell - 2\ell^2 + z - 2\ell z + 2\ell^2 z}. \end{cases} \tag{85}$$

To compare the two schemes, we define

$$\begin{cases} \epsilon_{ST} = |R_{staircase} - R_{continuous}| = \left|z^{2\ell} - 1\right| \\ \epsilon_{FD} = |R_{fictitious\,domain} - R_{continuous}|\,. \end{cases} \tag{86}$$

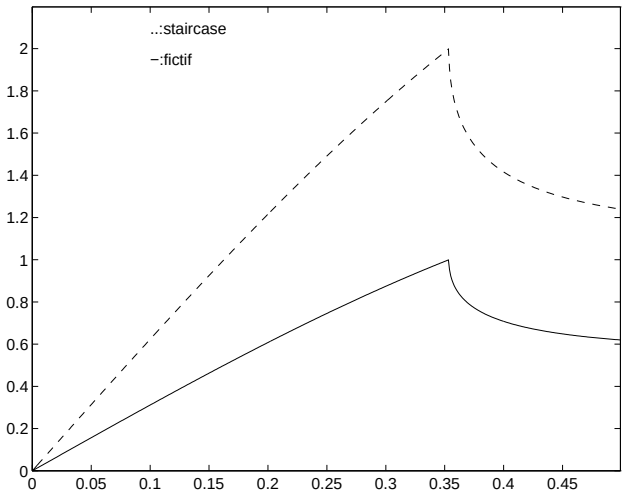

Fig 23: *errors of the reflection coefficient (- - -: staircase and - : fictitious case) versus the inverse of points per wavelength*

A Taylor expansion provides

$$\begin{cases} \epsilon_{ST} = 2\ell\omega h + O\left((\omega h)^2\right) \\ \epsilon_{FD} = 2\ell(1-\ell)\omega h + O\left((\omega h^2)\right). \end{cases} \tag{87}$$

As a result, both methods are first order with respect to ωh. Note that the transmission coefficient T is also first order with respect to ωh. However, since $2\ell(1-\ell) \leq 2\ell$, the error is smallest for the fictitious domain method than for the staircase approximation method especially when ℓ approaches $1/2$. This is confirmed by the curves of the figure 20 which compares the errors of the two approachs for different discretizations.

In Figure (20) is shown the variation of the errors versus the inverse of the number of points per wavelength. The Courant number $\Delta t/h$ is $1/\sqrt{2}$ and the location of the point x_ℓ corresponds to $h/2$ ($\ell = 1/2$). Although the fictitious method remains first order with respect to the discretization steps , it clearly improves the precision of the reflection coefficient.

Remark: It is easy to see that if $\ell = \frac{1}{2}$, the reflection coefficient obtained

from the fictitious method is one half of the one obtained using the staircase like approximation.

Unité de recherche INRIA Lorraine, Technopôle de Nancy-Brabois, Campus scientifique,
615 rue du Jardin Botanique, BP 101, 54600 VILLERS LÈS NANCY
Unité de recherche INRIA Rennes, Irisa, Campus universitaire de Beaulieu, 35042 RENNES Cedex
Unité de recherche INRIA Rhône-Alpes, 655, avenue de l'Europe, 38330 MONTBONNOT ST MARTIN
Unité de recherche INRIA Rocquencourt, Domaine de Voluceau, Rocquencourt, BP 105, 78153 LE CHESNAY Cedex
Unité de recherche INRIA Sophia-Antipolis, 2004 route des Lucioles, BP 93, 06902 SOPHIA-ANTIPOLIS Cedex

Éditeur
INRIA, Domaine de Voluceau, Rocquencourt, BP 105, 78153 LE CHESNAY Cedex (France)
ISSN 0249-6399